Available online at www.sciencedirect.com
SCIENCE DIRECT®
Pergamon
Cement and Concrete Research 34 (2004) 1251–1257
CEMENT AND CONCRETE RESEARCH

Calcium silicate structure and carbonation shrinkage of a tobermorite-based material

Fumiaki Matsushita[a,*], Yoshimichi Aono[b], Sumio Shibata[b]

[a]*Research and Development Center, Mie Branch, Sumitomo Metal Mining Siporex Co., Ltd, 1117-11, Ege, Seki-cho, Suzuka-gun, Mie, 519-1106, Japan*
[b]*Research and Development Center, Sumitomo Metal Mining Siporex Co., Ltd, 5-11-3, Shinbashi, Minato, Tokyo, 105-0004, Japan*

Received 17 March 2003; accepted 15 December 2003

Abstract

Carbonated autoclaved aerated concretes (AACs) show no shrinkage at a degree of carbonation approximately less than 20%. The ^{29}Si MAS NMR spectrum showed that at a degree of carbonation less than 25%, the typical double-chain silicate anion structure of tobermorite-11Å was well maintained and interlayer Ca ions were exchanged with protons. This corresponded to the absence of carbonation shrinkage at a degree of carbonation less than 20%. When the degree of carbonation increased from 25% to 50% up to 60%, the double-chain silicate anion structure of tobermorite-11Å was decomposed and Ca ions in the Ca–O layers were dissolved, showing a possible mechanism of carbonation shrinkage.

Keywords: Carbonation; Shrinkage; Degradation; Durability; Tobermorite

1. Introduction

One of the most harmful factors affecting the durability of autoclaved aerated concrete (AAC) is carbonation, in which tobermorite-11Å ($5CaO{\cdot}6SiO_2{\cdot}5H_2O$), the principal binding mineral of AAC, reacts with atmospheric carbon dioxide gas in the presence of moisture, and decomposes to silica gel and calcium carbonate as shown in Eq. (1).

$$5CaO \cdot 6SiO_2 \cdot 5H_2O + 5CO_2 \rightarrow 5CaCO_3 + 6SiO_2 + 5H_2O \quad (1)$$

Carbonation leads to degradation such as the decrease of strength, the increase of deflection and the growth of latticelike cracking [1,2], which are mainly caused by the carbonation shrinkage.

In the microstructure change of AAC during carbonation [3], the planer particle shapes of tobermorite-11Å and the associated interparticle pores were not changed significantly, although the double-chain silicate anion structure of tobermorite-11Å was decomposed to silica-gel-like structure, and drying shrinkage increased with carbonation.

Numerical values of carbonation shrinkage of AAC were reported from 0.1% to 1.0% for laboratory carbonation, although it varied according to the raw materials, carbon dioxide concentration and relative humidity (RH) [4–8].

However, the relationship between carbonation shrinkage and change of tobermorite-11Å crystal structure has not been reported. We studied the mechanism of carbonation shrinkage of AAC, carbonated under an accelerated condition, with ^{29}Si MAS NMR spectroscopy. We also studied the carbonation shrinkage of AAC carbonated under field conditions, which is extremely difficult to measure.

2. Experimental

2.1. Specimens

AAC blocks made by Sumitomo Metal Mining Siporex were used for laboratory carbonation. The $40 \times 40 \times 160$-mm blocks were dried at 105 °C for 2 h. After that, a pair of 20-mm brass pins was fixed on both ends by an adhesive for the length change measurement. A surface part from 0 to 10 mm was used for determining the degree of carbonation.

Field AAC wall panels under working conditions for 9, 26 and 33 years were used as field-carbonated samples.

* Corresponding author. Tel.: +81-5959-6-1131; fax: +81-5959-6-1987.
E-mail address: Fumiaki_Matsushita@ni.smm.co.jp (F. Matsushita).

0008-8846/$ – see front matter © 2004 Elsevier Ltd. All rights reserved.
doi:10.1016/j.cemconres.2003.12.016

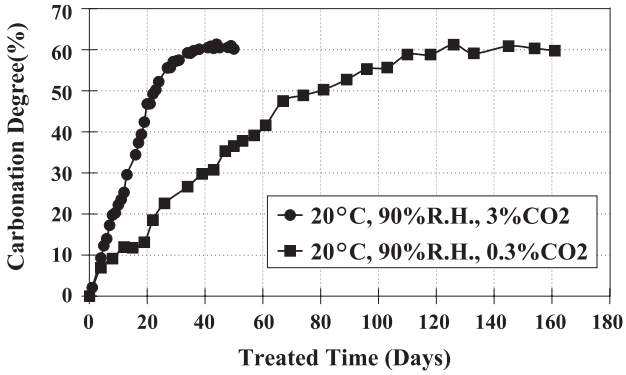

Fig. 1. Degree of carbonation as a function of treated days.

Degree of carbonation of the specimens was approximately 25%, 50% and 60%, respectively.

2.2. Carbonation

Laboratory carbonation samples were pretreated at a temperature of 20 °C and 90% RH for 1 week. Subsequently, they were carbonated under conditions of CO_2 concentration of 3 and 0.3 vol.%, temperature of 20 °C and an ambient RH of 90%.

2.3. Degree of carbonation [9]

The amount of combined carbon dioxide and calcium oxide was measured to determine the degree of carbonation. TG-DTA was used for determining the amount of combined carbon dioxide except for the amount of adsorbed carbon dioxide gas and carbonated salt other than calcium carbonate. The amount of combined carbon dioxide was measured as the weight loss during heating from 600 to 800 °C, corresponding to the decomposition of calcium carbonate. The amount of calcium oxide was determined by ICP. The degree of carbonation (D_c) can be given by

$$D_c\ (\%) = [(C - C_0)/(C_{max} - C_0)] \times 100, \quad (2)$$

where C, C_0 and C_{max} are the amount of combined carbon dioxide in a sample, that of an untreated AAC and that when all calcium oxide transformed to calcium carbonate, respectively. Degree of carbonation for field-carbonated specimens was calculated, with $C_0 = 1.0\%$ as a generally acceptable value.

2.4. Carbonation shrinkage

Shrinkage strain δ due to carbonation can be given by

$$\delta = [(I - I_0)/I_0] \times 100, \quad (3)$$

where I and I_0 are current length and initial length, respectively, after pretreatment under conditions of 20 °C and 90% RH for 1 week. Measurement was always done in the carbonation chamber under conditions of 20 °C and 90% RH.

2.5. ^{29}Si MAS NMR spectra

^{29}Si MAS NMR spectra were recorded by a Jeol JNM-Λ-400WB with an observation frequency of 79.42 MHz, a repeating time of 7.0 s, a contact time of 6.4 μs and a cumulative number of 3000 to 12,000 scans. The specimens measured were untreated AAC and laboratory- and field-carbonated AAC with degrees of carbonation of 25%, 50% and 60%, respectively.

3. Results and discussion

3.1. Degree of carbonation

Degree of carbonation as a function of treated days is shown in Fig. 1. The higher the carbon dioxide concentration, the faster the increase in degree of carbonation. Degree of carbonation reached saturation approximately at 60% after 35 days under a CO_2 concentration of 3 vol.% and 120 days under a CO_2 concentration of 0.3 vol.%.

3.2. Carbonation shrinkage

Carbonation shrinkage reached approximately 0.25% after 40 days at a CO_2 concentration of 3 vol.% and after 160 days at 0.3 vol.% CO_2, showing that higher CO_2 concentration led to a quicker shrinkage (Fig. 2). The maximum value of carbonation shrinkage was approximately 0.27% at 3 vol.% CO_2 concentration and approximately 0.25% at 0.3 vol.% CO_2.

Besides the decomposition of tobermorite-11Å, calcium carbonate was deposited during carbonation. The absence of swelling during carbonation was attributed to the deposition of calcium carbonate into the interparticle pores [3].

Length change during carbonation as a function of the degree of carbonation is shown in Fig. 3. Regardless of

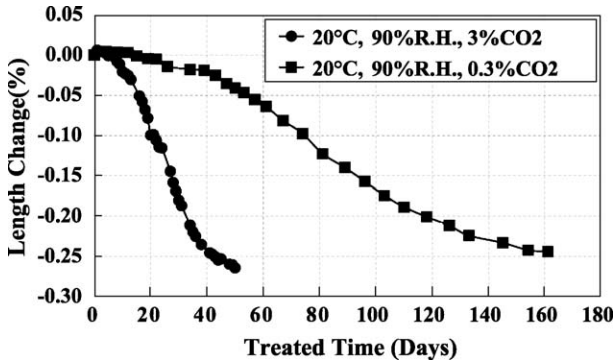

Fig. 2. Length change during laboratory carbonation as a function of treated days.

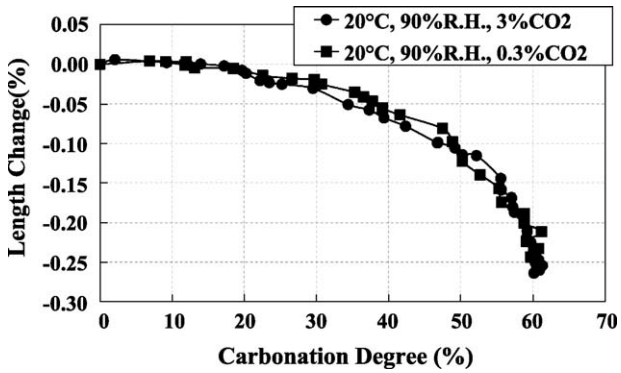

Fig. 3. Length change during laboratory carbonation as a function of degree of carbonation.

carbonation conditions the relationship between degree of carbonation and carbonation shrinkage showed nearly the same tendency. Carbonation shrinkage did not occur when the degree of carbonation was less than 20%. When the degree of carbonation ranged from 20% to 50%, carbonation shrinkage occurred gradually and reached approximately 0.1%. When the degree of carbonation ranged from 50% to 60%, significant carbonation shrinkage occurred and reached approximately 0.25%.

3.3. ^{29}Si MAS NMR spectrum

^{29}Si MAS NMR spectra of untreated AAC and laboratory- and field-carbonated AAC with degrees of carbonation

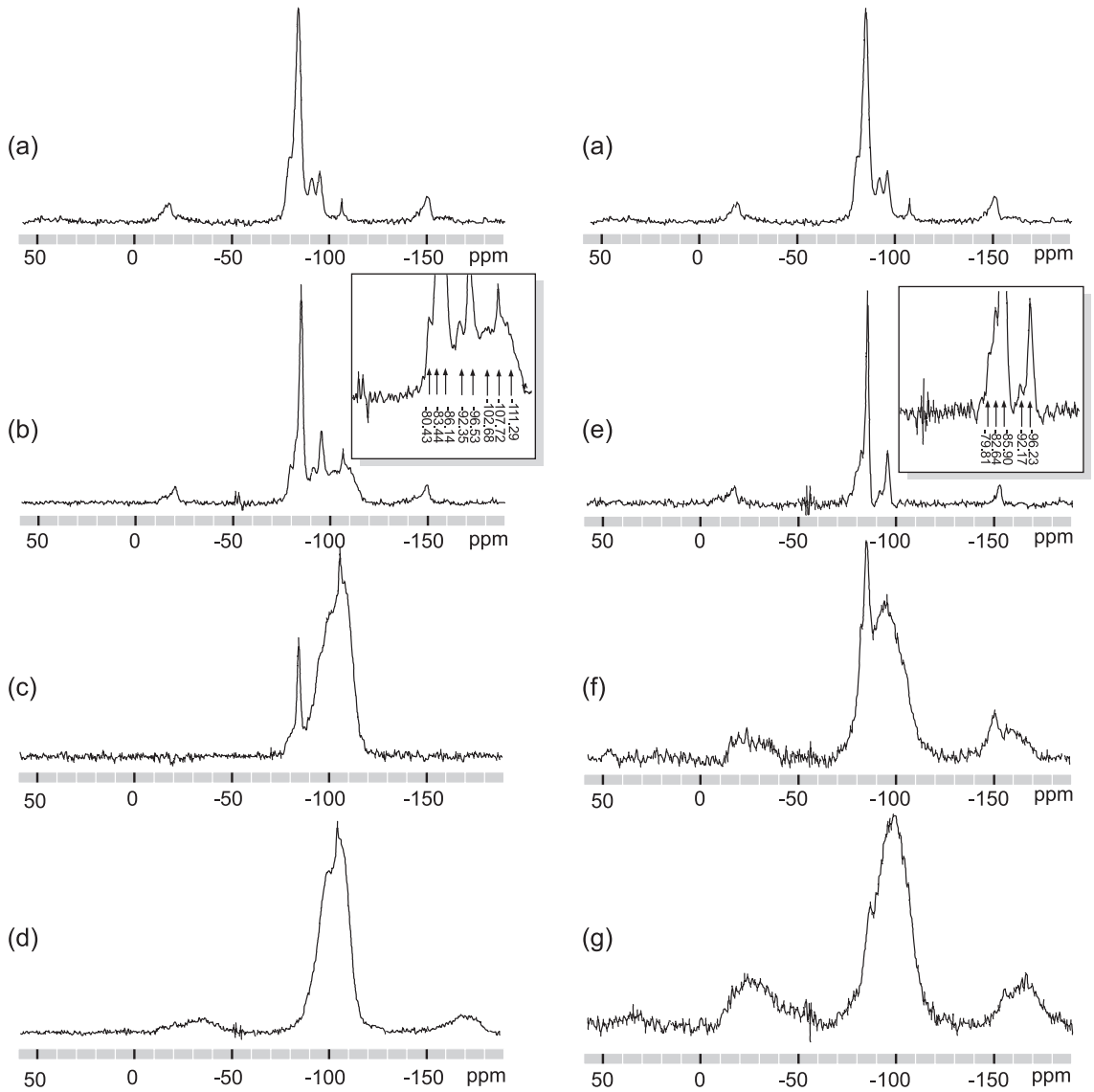

Fig. 4. ^{29}Si MAS NMR spectrum. (a) Untreated AAC; (b) laboratory-carbonated AAC, D_c = 25%; (c) laboratory-carbonated AAC, D_c = 50%; (d) laboratory-carbonated AAC, D_c = 60%; (e) field-carbonated AAC, D_c = 25%; (f) field-carbonated AAC, D_c = 50%; (g) field-carbonated AAC, D_c = 60%.

of 25%, 50% and 60%, respectively, are shown in Fig. 4(a) to (g). The ^{29}Si MAS NMR chemical shifts by peak separation are shown in Table 1.

On the whole, changes of silicate anion structures of laboratory- and field-carbonated specimens were the same. When the degree of carbonation was less than 25%, ^{29}Si MAS NMR spectra were almost unchanged, which implied the double-chain silicate anion structure of tobermorite-11Å was well maintained; however, at peaks around −100 ppm a little change was observed in laboratory-carbonated specimens (Fig. 4(a), (b) and (e)). On the other hand, at the same progress of degree of carbonation of 25%, ^{29}Si MAS NMR spectra of specimens with a degree of carbonation ranging from 25% to 50% changed considerably (Fig. 4 (c) and (f)). Furthermore, when the degree of carbonation ranged from 50% to 60%, ^{29}Si MAS NMR spectra changed remarkably in spite of only 10% increase in the degree of carbonation (Fig. 4 (d) and (g)). During this process, the double-chain silicate anion structure of tobermorite-11Å (Q2 and Q3) was supposed to be rearranged to a 3-D silica-gel-like structure (Q4).

3.3.1. Untreated specimens

For untreated AAC, signals at −80.6, −85.3, −92.0, −96.0 and −107.4 ppm were observed, which corresponded to Q1, Q2, Q3(1Al) Q3(0Al) and Q4, respectively [10,11]. Q4 signal at −107.3 ppm corresponded to α-quartz, one of the raw materials of AAC. The value of Q3/Q2 of the untreated specimen was approximately 1/3, although the theoretical value is 1/2. Therefore, the bridging tetrahedra were supposed to comprise ∼25% of Q2 and ∼75% of Q3. We call the Q2 at the bridging tetrahedra Q2b in this paper.

3.3.2. Carbonation degree of 25%

When the degree of carbonation reached 25%, signals at −83.4, −102.7 and −111.3 ppm appeared in the laboratory-carbonated specimen, and a signal at −82.6 ppm appeared in the field-carbonated specimen. The signal at −111.3 ppm corresponds to Q4 of silica gel [12], which differs from Q4 of α-quartz (−107 ppm). Sato and Grutzeck [13] and Sasaki et al. [14] concluded from the ^{29}Si MAS/CPMAS NMR spectrum that the signal around −82 ppm corresponded to the protonated silicate ions in the silicate chain. Klur et al. [15] proposed to attribute the signal around −82.1 ppm to bridging tetrahedra bonded to two protons (Q2p), −83.9 ppm to bridging tetrahedra bonded to one proton and one calcium ion (Q2i), and −85.3 ppm to silicate tetrahedra coordinated to the calcium ions (Q2Ca). In short, Q2Ca designated by Klur et al. means the ordinary Q2. Therefore, the signal at −83.4 ppm for laboratory-carbonated specimen and at −82.6 ppm for field-carbonated specimen corresponded to Q2i and Q2p, respectively. A signal at −102.7 ppm corresponds to the bridging tetrahedra bonded to one proton and one silicate ion, Q3(1OH). [16] The tobermorite-structure model including Q3(1OH), Q2b, Q2p, Q2i and Q2Ca bonds is shown in Fig. 5. The appearance of Q2p, Q2i and Q3(1OH) including the protonated silicate ions during the early carbonation periods signified the exchange of calcium ions by protons in the interlayer space of tobermorite-11Å.

3.3.3. Carbonation degree more than 50%

When the degree of carbonation reached 50%, Q1 disappeared, Q2 peaks around −82 to −86 ppm became relatively lower and Q3 and Q4 appeared or increased in both carbonated specimens. For laboratory-carbonated specimens, Q2i (−83.4 ppm) disappeared, a slight signal of Q2p (−82.8 ppm) appeared and the highest signal changed from Q2 to Q4. For field-carbonated specimens, Q3(1Al) (−92.2 ppm) disappeared, Q3(1OH) (−103.9 ppm) appeared and the highest signal changed from Q2 to Q3.

When the degree of carbonation reached 60%, Q3(1OH) and Q4 were detected for laboratory-carbonated specimens. On the other hand, the wide signal centered between Q3 and

Table 1
^{29}Si MAS NMR chemical shifts of sample

ppm from TMS (relative intensity)	Q1	Q2			Q3			Q4	
		Q2p	Q2i	Q2Ca	Q3(1A1)	Q3	Q3(1OH)	Q4	Q4(quartz)
Untreated	−80.6 (28)			−85.3 (100)	−92.0 (16)	−96.0 (17)			−107.4 (4)
Laboratory-carbonated, D_c = 25%	−80.4 (15)		−83.4 (51)	−86.1 (100)	−92.4 (23)	−96.5 (42)	−102.7 (54)	−111.3 (48)	−107.7 (14)
Laboratory-carbonated, D_c = 50%		−82.8 (5)		−86.1 (21)		−98.0 (60)	−102.3 (90)	−111.1 (100)	−107.7 (15)
Laboratory-carbonated, D_c = 60%							−102.8 (100)	−110.3 (68)	−107.5 (5)
Field-carbonated, D_c = 25%	−79.8 (12)	−82.6 (30)		−85.9 (100)	−92.2 (3)	−96.2 (28)			
Field-carbonated, D_c = 50%		−82.9 (13)		−86.0 (48)		−96.9 (100)	−103.9 (60)		
Field-carbonated, D_c = 60%				−87.2 (29)	−98.9 (100)	−98.9 (100)	−98.9 (100)	−98.9 (100)	

TMS = tetramethylsilane.

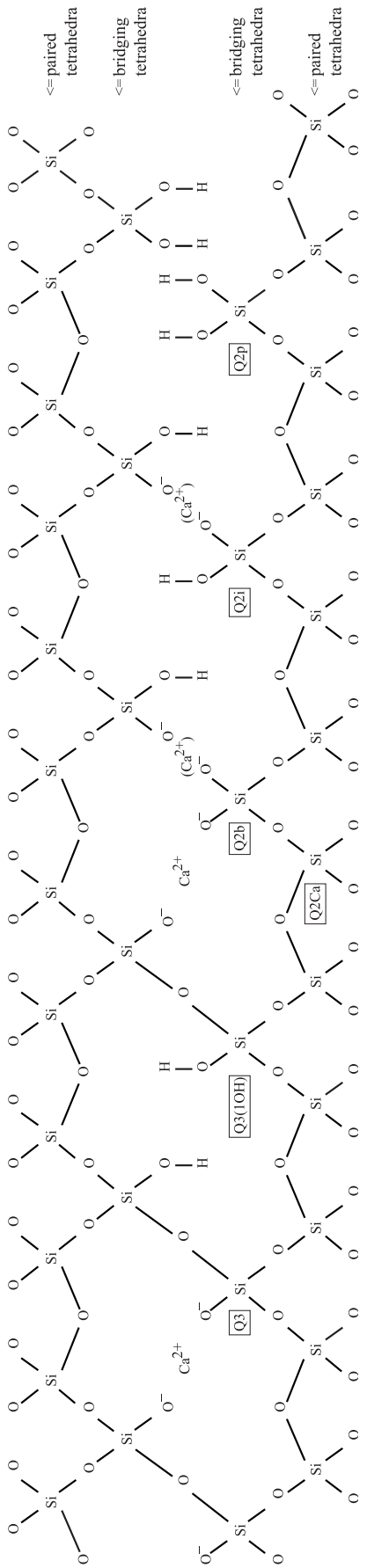

Fig. 5. The tobermorite structure model including Q3(1OH), Q2b, Q2p, Q2i and Q2Ca bonds.

Q4 was mainly detected for field-carbonated specimen. Therefore, the double-chain silicate anion structure of tobermorite-11Å was finally decomposed, shrunk and polymerized to a silica-gel-like structure in the final stage of carbonation.

3.4. Changes of silicate anion structures and carbonation shrinkage

During the early carbonation periods at a degree of carbonation less than 25%, the double-chain silicate anion structure of tobermorite-11Å was well maintained and protonated silicate ions in the silica chain appeared for both types of specimen. Komarneni and Tsuji [17] studied the ion exchange properties of Ca ions in the interlayer space of tobermorite-11Å. The Ca ions in the interlayer and the Ca–O layer composed 20% and 80% of Ca atoms in tobermorite-11Å, respectively [18]. In the case of laboratory-carbonated specimens, carbonation shrinkage did not occur when the degree of carbonation was less than 20%. Therefore, the absence of carbonation shrinkage until the degree of carbonation of 20% may be attributed to the retaining of the main structures of tobermorite-11Å, the double-chain silicate anion structure and the Ca–O layer.

During the carbonation periods, at degree of carbonation from 25% to 60%, Ca ions dissolved from the Ca–O layer and the double-chain silicate anion structure decomposed, shrunk and polymerized to a silica gel structure. This is the most likely mechanism of carbonation shrinkage of AAC, a tobermorite-based material. It can also support the relation that both the progress of carbonation shrinkage and the change of silicate anion structure when the degree of carbonation ranged from 50% to 60% were more remarkable than that when the degree of carbonation ranged from 20% or 25% to 50%.

For field-carbonated specimens, measurement of carbonation shrinkage for several decades was extremely difficult. In this study, changes of silicate anion structures for field and laboratory carbonation turned out to be very similar. Therefore, carbonation shrinkage of field-carbonated specimens, as a function of degree of carbonation, was supposed to be the same as that of laboratory-carbonated specimens.

4. Conclusion

1. For laboratory-carbonated specimens under CO2 concentrations of 3 and 0.3 vol.%, the relationship between the degree of carbonation and carbonation shrinkage was nearly the same. Carbonation shrinkage was not observed when the degree of carbonation was less than 20%. Carbonation shrinkage reached approximately 0.1% and 0.25% at a degree of carbonation of 50% and 60%, respectively.
2. When the degree of carbonation was less than 25%, ^{29}Si MAS NMR spectrum suggested that the double-chain silicate anion structure of tobermorite-11Å was well maintained and calcium ions were exchanged by protons. It was suggested the absence of carbonation shrinkage until the degree of carbonation of 20% was reached could be due to the retaining of the double-chain silicate anion structure and the Ca–O layer, the main structures of tobermorite-11Å.
3. When the degree of carbonation ranged from 25% to 60%, Ca ions dissolved from the Ca–O layer and the double-chain silicate anion structures were decomposed, shrunk and were polymerized to silica-gel-like structure. This is the most likely mechanism of carbonation shrinkage of AAC, a tobermorite-based material.
4. Carbonation shrinkage of field-carbonated specimens as a function of degree of carbonation was supposed to be the same as that of laboratory-carbonated specimens, because changes of silicate anion structures of field and laboratory-carbonated specimens were very similar.

Acknowledgements

The authors are grateful to Prof. Dr. Wolfgang Wieker of Witega, Berlin, Germany for private discussions.

References

[1] A. Goodier, S. Matthews, In-service behavior of reinforced autoclaved aerated concrete planks, No. SP-170, Spec. Publ. Am. Concr. Inst. 2 (1997) 1197–1214.
[2] F. Matsushita, S. Shibata, Carbonation degree as durability criteria for autoclaved aerated concrete, in: V.M. Malhotra (Ed.), 5th CANMET/ACI International Conference on Durability of Concrete, Am. Concr. Inst., ACI, Michigan, No. SP-192, 2000, pp. 1123–1134.
[3] F. Matsushita, S. Shibata, Y. Aono, T. Kamada, Microstructure of autoclaved aerated concrete subjected to carbonation, in: M. Lacasse D.J. Vanier (Eds.), 8th International Conference on Durability of Building Materials and Components, NRC Research Press, Ottawa, 1999, pp. 159–169.
[4] Z. Sauman, Effect of CO_2 on porous concrete, Cem. Concr. Res. 2 (1972) 541–549.
[5] A.A. Fedin, E.M. Chernyshov, E.M. Ponomareva, Stability of silicate aerated concrete during carbonatation, Tr. Probl. Lab. Silikat. Mater. Konstr., Voronezh. Inzh.-Stroit. Inst. 4 (1970) 31–43 (in Russian).
[6] L.N. Novikova, A.B. Ustimovich, Z.V. Stankevich, T.L. Minchukova, Effect of artificial carbonization on the properties and structure of newly formed phases in cellular concrete with reduced bulk density, Stroit. Mater. 6 (1978) 32–33 (in Russian).
[7] T. Nireki, H. Kabeya, N. Hirama, T. Inoue, Durability of aerated lightweight concrete panels with surface coating systems, Durability of Building Materials and Components, E&FN Spon, London, 1990, pp. 721–727.
[8] T. Ochiai, Carbonation of autoclaved light-weight concretes, Gypsum and Lime 242 (1993) 22–31 (in Japanese).
[9] F. Matsushita, Y. Aono, S. Shibata, Carbonation degree of autoclaved aerated concrete, Cem. Concr. Res. 30 (2000) 1741–1745.
[10] W. Wieker, A.-R. Grimmer, A. Winkler, M. Magi, M. Tarmak, E. Lippmaa, Solid-state high-resolution 29Si NMR spectroscopy of synthetic 14Å, 11and 9Å tobermorites, Cem. Concr. Res. 12 (1982) 333–339.

[11] S. Komarneni, R. Roy, D.M. Roy, C.A. Fyfe, G.J. Kennedy, A.A. Bother-by, J. Dadok, A.S. Chesnick, 27Al and 29Si magic angle spinning nuclear magnetic resonance spectroscopy of al-substituted tobermorites, J. Mater. Sci. 20 (1985) 4209–4214.
[12] A.R. Grimmer, P. Starke, W. Wieker, M. Maegi, High resolution solid-state silicon-29 NMR of silica gels, Z. Chem. 22 (2) (1982) 44 (in German).
[13] H. Sato, M. Grutzeck, Effect of starting materials on the synthesis of tobermorite, Mater. Res. Soc. Symp. Proc. 245 (1992) 235–240.
[14] K. Sasaki, T. Masuda, H. Ishida, T. Mitsuda, Structural degradation of tobermorite during vibratory milling, J. Am. Ceram. Soc. 79 (6) (1996) 1569–1574.
[15] I. Klur, B. Pollet, J. Virlet, A. Nonat, C-S-H structure evolution with calcium content by multinuclear NMR, in: P. Colombet, A.-R. Grimmer H. Zanni, P. Sozzani (Eds.), Nuclear Magnetic Resonance Spectroscopy of Cement-Based Materials, Springer, Berlin, 1997, pp. 119–141.
[16] X.-D. Cong, R.J. Kirkpatrick, S. Diamond, 29Si MAS NMR spectroscopic investigation of alkali silica reaction product gels, Cem. Concr. Res. 23 (4) (1993) 811–823.
[17] S. Komarneni, M. Tsuji, Selective cation exchange in substituted tobermorites, J. Am. Ceram. Soc. 72 (9) (1989) 668–1674.
[18] H.F.W. Taylor, The Chemistry of Cements, Academic Press, London, 1964, pp. 185–189, (chapter 5).